Numerical Simulation of Flow in Helical Ducts

Jing-Wu Wang and J. R. G. Andrews
Dept. of Chemical Engineering, Monash University, Clayton, Victoria 3168, Australia

Helical pipes and ducts are used widely in industry. There is a huge literature on flow in curved pipes and bends, but comparatively little has been published on flow in helical pipes. To simplify the problem, most theoretical work on flow in helical pipes has assumed zero pitch: a toroidal pipe following the work of Dean in 1927. Recent theoretical studies on helical pipes have used helical coordinate systems. These systems, however, are not appropriate when studying helical ducts. The following results are reported: a coordinate system appropriate for helical ducts; the detailed equations of continuity and motion in this coordinate system; the numerical method used to find the fully developed laminar flow of a Newtonian liquid in helical ducts; the simulations vs. published experimental data; and effects of the pitch ratio, curvature ratio and pressure gradient on secondary flow in a helical duct.

Introduction

Fluid flow in a helical pipe or duct is encountered in many industrial situations. The most important characteristic of such flow is secondary flow, the flow circulating cross-sectionally. The secondary flow is superimposed upon the helical flow. It not only changes the velocity profile of the flow in a helical duct, but also the flow resistance and pressure drop as compared to a straight duct. Fundamental research on the velocity distribution and flow resistance in a helical duct is important in the fields of chemical, mechanical, and civil engineering.

The secondary flow occurs in curved pipes or curved ducts. Dean (1927, 1928) was the first to introduce a toroidal coordinate system to investigate the pressure-driven laminar flow of an incompressible Newtonian fluid in a curved pipe with a circular cross section. Since then most researchers have adopted Dean's toroidal coordinates in their studies. Comprehensive reviews on flow in curved pipes have been written by Ward-Smith (1980), Berger et al. (1983), and Ito (1987). Comparatively little, however, is known about flow in helical pipes. In the review article by Berger et al. (1983), there were over a hundred references to flow in toroidally curved pipes, but only four articles on helical pipe flow (Austin and Seader, 1973; Joseph et al., 1975; Joseph and Adler, 1975). The authors of these articles all used toroidal coordinate system when simulating flow in helical pipes and ducts.

Wang (1981) pointed out that toroidally curved pipes only involve a curvature c_u, but helical pipes have both curvature c_u and torsion t_o

$$c_u = \frac{R}{R^2 + a^2} \qquad t_o = \frac{a}{R^2 + a^2}$$

where R is the internal radius of helical duct and a is a constant in the helical coordinate system, $a = \text{Pitch}/2\pi$.

If the pitch is equal to zero, the torsion t_o is equal to zero and the helical pipe reduces to the toroidally curved pipe. Since the authors of the four articles just cited all calculated the flow in helical pipes using toroidal coordinate systems, what they were in fact doing was computing flow in a toroidal pipe instead of the flow in a helical pipe. The effect of torsion on flow cannot appear in their calculation. Kao (1987) suggested that the torsion can radically change the pattern of the secondary flow in a helical pipe, although the influence of torsion on the volume flux ratio is relatively minor.

Some of the more recent theoretical articles on helical pipes (Wang, 1981; Germano, 1982, 1989; Huang and Gu, 1989) have used helical coordinates, although only the coordinate system described by Huang and Gu (1989) is appropriate for helical ducts. This article does not give the detailed equations of continuity and motion in helical coordinates.

The present article provides a comprehensive study of the effect of the pitch ratio, pressure gradient, and curvature ratio on the velocity distribution and fluid resistance in fully developed laminar flow of an incompressible fluid in a helical duct with a rectangular cross section.

Correspondence concerning this article should be addressed to J.-W. Wang.

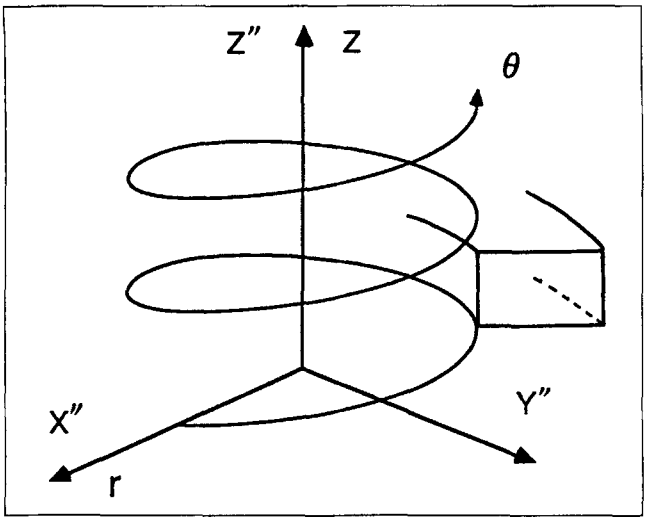

Figure 1. Helical coordinate system.

Helical Coordinate System

A coordinate system that is suitable for describing flow in a helical duct (with a rectangular cross section) is the helical coordinate system, as shown in Figure 1, which is a nonorthogonal system. When the pitch is equal to zero, the helical coordinate system reduces to the standard cylindrical coordinates. To develop a nonorthogonal coordinate system, a tensor analysis is needed.

The Cartesian coordinates can be expressed in the form of

$$Y^i = (x'', y'', z'')$$

and the helical coordinates are expressed as

$$X^i = [r, \theta, z].$$

The helical coordinates X^i are defined as having the following relations to the Cartesian coordinates Y^i

$$x'' = r\cos\theta \qquad y'' = r\sin\theta \qquad z'' = z + a\theta. \tag{1}$$

The metric tensor g_{ij} and g^{ij} for the helical coordinate system can be expressed as

$$g_{ij} = \begin{bmatrix} 1 & 0 & 0 \\ 0 & r^2+a^2 & a \\ 0 & a & 1 \end{bmatrix} \quad g^{ij} = \begin{bmatrix} 1 & 0 & 0 \\ 0 & \dfrac{1}{r^2} & -\dfrac{a}{r^2} \\ 0 & -\dfrac{a}{r^2} & \dfrac{r^2+a^2}{r^2} \end{bmatrix}. \tag{2}$$

Since g_{ij} and g^{ij} have nonzero off-diagonal elements, the helical coordinate system in the present study is not orthogonal.

Aris (1962) defined the Christoffel symbol of the first kind:

$$[jk, i] = \frac{1}{2}\left(\frac{\partial g_{ij}}{\partial x^k} + \frac{\partial g_{ik}}{\partial x^j} - \frac{\partial g_{jk}}{\partial x^i}\right).$$

The nonzero Christoffel symbols of the first kind for the helical coordinate system are

$$[1\,2, 2] = [2\,1, 2] = r \qquad [2\,2, 1] = -r,$$

which are the same expressions as the nonzero Christoffel symbols of the first kind for the standard cylindrical coordinate system given by Eringen (1967).

Aris (1962) defined the Christoffel symbols of the second kind as

$$\left\{ \begin{matrix} i \\ jk \end{matrix} \right\} = g^{il}[jk, l].$$

The nonzero Christoffel symbols of the second kind for the helical coordinate system are

$$\left\{ \begin{matrix} 1 \\ 2\,2 \end{matrix} \right\} = -r \qquad \left\{ \begin{matrix} 2 \\ 1\,2 \end{matrix} \right\} = \left\{ \begin{matrix} 2 \\ 2\,1 \end{matrix} \right\} = \frac{1}{r}$$

$$\left\{ \begin{matrix} 3 \\ 1\,2 \end{matrix} \right\} = \left\{ \begin{matrix} 3 \\ 2\,1 \end{matrix} \right\} = -\frac{a}{r}.$$

If a is equal to zero, Eqs. 1 and 2 and the nonzero Christoffel symbols can be used to transform the Cartesian coordinates to the cylindrical coordinates given by Eringen (1967).

Wang (1981) expressed the equation of continuity and the equations of motion in tensor form as follows:

$$\frac{\partial v^i}{\partial x^i} + \left\{ \begin{matrix} i \\ k\,i \end{matrix} \right\} v^k = 0 \tag{3}$$

$$\frac{\partial v^i}{\partial t} + v^j\left(\frac{\partial v^i}{\partial x^j} + \left\{ \begin{matrix} i \\ k\,j \end{matrix} \right\} v^k\right) = -\frac{g^{ij}}{\rho}\frac{\partial p}{\partial x^j} + f^i + \nu g^{kj} v^i_{,jk}. \tag{4}$$

Here the covariant derivative is

$$v^i_{,jk} = \left[\frac{\partial^2 v^i}{\partial x^j \partial x^k} + \left\{ \begin{matrix} i \\ l\,j \end{matrix} \right\}\frac{\partial v^l}{\partial x^k} + \left\{ \begin{matrix} i \\ l\,k \end{matrix} \right\}\frac{\partial v^l}{\partial x^j} - \left\{ \begin{matrix} l \\ j\,k \end{matrix} \right\}\frac{\partial v^i}{\partial x^l} + \left(\frac{\partial}{\partial x^k}\left\{ \begin{matrix} i \\ m\,j \end{matrix} \right\} + \left\{ \begin{matrix} i \\ l\,k \end{matrix} \right\}\left\{ \begin{matrix} l \\ m\,j \end{matrix} \right\} - \left\{ \begin{matrix} l \\ j\,k \end{matrix} \right\}\left\{ \begin{matrix} i \\ m\,l \end{matrix} \right\}\right) v^m\right].$$

In the application of the equations in tensor forms to specific problems, the vector components v^i are replaced by the physical components $v^{(i)}$ of the vector **v**. Eringen (1967) defined the physical components $v^{(i)}$ related to the vector components v^i as

$$v^{(i)} = v^i\sqrt{g_{ii}} \qquad v^i = \frac{v^{(i)}}{\sqrt{g_{ii}}}$$

where $\sqrt{g_{ii}} = |\mathbf{g}_i|$.

By substituting the physical components $v^{(i)}$ for the vector components v^i, Eq. 3 and Eq. 4 become

$$\frac{\partial}{\partial x^i}\left(\frac{v^{(i)}}{\sqrt{g_{ii}}}\right)+\left\{\begin{matrix} i \\ k\,i \end{matrix}\right\}\left(\frac{v^{(k)}}{\sqrt{g_{kk}}}\right)=0 \tag{5}$$

$$\frac{\partial v^{(i)}}{\partial t}+\sqrt{g_{ii}}\left(\frac{v^{(j)}}{\sqrt{g_{jj}}}\right)\left[\frac{\partial}{\partial x^j}\left(\frac{v^{(i)}}{\sqrt{g_{ii}}}\right)+\left\{\begin{matrix} i \\ k\,j \end{matrix}\right\}\left(\frac{v^{(k)}}{\sqrt{g_{kk}}}\right)\right]$$
$$=-\frac{\sqrt{g_{ii}}}{\rho}g^{ij}\frac{\partial p}{\partial x^j}+f^{(i)}+\nu\sqrt{g_{ii}}g^{kj}v^{(i)}_{,jk}. \tag{6}$$

Here the covariant derivative is

$$v^{(i)}_{,jk}=\left[\frac{\partial^2}{\partial x^j\partial x^k}\left(\frac{v^{(i)}}{\sqrt{g_{ii}}}\right)+\left\{\begin{matrix} i \\ l\,j \end{matrix}\right\}\frac{\partial}{\partial x^k}\left(\frac{v^{(l)}}{\sqrt{g_{ll}}}\right)+\left\{\begin{matrix} i \\ l\,k \end{matrix}\right\}\frac{\partial}{\partial x^j}\left(\frac{v^{(l)}}{\sqrt{g_{ll}}}\right)-\left\{\begin{matrix} l \\ j\,k \end{matrix}\right\}\frac{\partial}{\partial x^l}\left(\frac{v^{(i)}}{\sqrt{g_{ii}}}\right)$$
$$+\left(\frac{\partial}{\partial x^k}\left\{\begin{matrix} i \\ m\,j \end{matrix}\right\}+\left\{\begin{matrix} i \\ l\,k \end{matrix}\right\}\left\{\begin{matrix} l \\ m\,j \end{matrix}\right\}-\left\{\begin{matrix} l \\ j\,k \end{matrix}\right\}\left\{\begin{matrix} i \\ m\,l \end{matrix}\right\}\right)\left(\frac{v^{(m)}}{\sqrt{g_{mm}}}\right)\Bigg].$$

Detailed Equations and Boundary Conditions

By substituting the metric tenors and the nonzero Christoffel symbols of the second kind for the corresponding terms in Eqs. 5 and 6, the detailed equation of continuity and the equations of motion in the nonorthogonal helical coordinate system are obtained.

Because the viscosity is a very important factor for adjusting the convergence of the numerical method that will be adapted, the viscosity should be an explicit term in dimensionless equations (Browne, 1978). The equation of continuity and the equations of motion can be made in a dimensionless form by introducing new variables defined as follows:

$$t=\frac{t'}{\sqrt{L/g_c}} \qquad r=\frac{r'}{L'} \qquad z=\frac{z'}{L'} \qquad \phi=\frac{\phi'}{g'_cL'}$$
$$\nu=\frac{\nu'}{\sqrt{g'_cL'^3}} \qquad u=\frac{u'}{\sqrt{g'_cL'}} \qquad v=\frac{v'}{\sqrt{g'_cL'}} \qquad w=\frac{w'}{\sqrt{g'_cL'}}$$
$$g_r=\frac{g'_r}{g'_c} \qquad g_\theta=\frac{g'_\theta}{g'_c} \qquad g_z=\frac{g'_z}{g'_c}$$

where the variables with prime notations are dimensional, L' is a characteristic length, and g'_c is a conversion factor.

Since the system is helically symmetrical, all the terms differentiated by θ are deleted except the term $\sqrt{r^2+a^2}\,\partial\phi/r^2\partial\theta$ in Eq. 9 and the term $a\partial\phi/r^2\partial\theta$ in Eq. 10 are kept. Equations of continuity and motion in dimensionless forms for modeling the flow in a helical duct are thus obtained

$$\frac{\partial u}{\partial r}+\frac{\partial w}{\partial z}+\frac{u}{r}=0 \tag{7}$$

$$\frac{\partial u}{\partial t}+u\frac{\partial u}{\partial r}+w\frac{\partial u}{\partial z}-\frac{rv^2}{r^2+a^2}=-\frac{\partial\phi}{\partial r}$$
$$+\nu\left(\frac{\partial^2u}{\partial r^2}+\frac{r^2+a^2}{r^2}\frac{\partial^2u}{\partial z^2}+\frac{2a}{r\sqrt{r^2+a^2}}\frac{\partial v}{\partial z}+\frac{1}{r}\frac{\partial u}{\partial r}-\frac{u}{r^2}\right) \tag{8}$$

$$\frac{\partial v}{\partial t}+u\frac{\partial v}{\partial r}+w\frac{\partial v}{\partial z}+\frac{2uv}{r}-\frac{ruv}{r^2+a^2}=\frac{a\sqrt{r^2+a^2}}{r^2}\frac{\partial\phi}{\partial z}$$
$$-\frac{\sqrt{r^2+a^2}}{r^2}\frac{\partial\phi}{\partial\theta}+\nu\left\{\frac{\partial^2v}{\partial r^2}+\left(\frac{3}{r}-\frac{2r}{r^2+a^2}\right)\frac{\partial v}{\partial r}\right.$$
$$+\left[\frac{3r^2}{(r^2+a^2)^2}-\frac{4}{r^2+a^2}\right]v+\frac{r^2+a^2}{r^2}\frac{\partial^2v}{\partial z^2}$$
$$\left.-\frac{2a\sqrt{r^2+a^2}}{r^3}\frac{\partial u}{\partial z}\right\} \tag{9}$$

$$\frac{\partial w}{\partial t}+u\frac{\partial w}{\partial r}+w\frac{\partial w}{\partial z}-\frac{2auv}{r\sqrt{r^2+a^2}}=-\frac{r^2+a^2}{r^2}\frac{\partial\phi}{\partial z}-\frac{a}{r^2}\frac{\partial\phi}{\partial\theta}$$
$$+\nu\left[\frac{\partial^2w}{\partial r^2}+\frac{r^2+a^2}{r^2}\frac{\partial^2w}{\partial z^2}-\frac{2a}{r\sqrt{r^2+a^2}}\frac{\partial v}{\partial r}\right.$$
$$\left.+\frac{2av}{\sqrt{(r^2+a^2)^3}}+\frac{2a^2}{r^3}\frac{\partial u}{\partial z}+\frac{1}{r}\frac{\partial w}{\partial r}\right]. \tag{10}$$

In the preceding equations, the centrifugal acceleration and Coriolis accelerations are not only a function of the velocities and radius but also a function of the pitch of the helical coordinates. There is an extra acceleration term $(2auv)/(r\sqrt{r^2+a^2})$ in the third equation of motion compared with that in a cylindrical coordinate system. If a is equal to zero, the preceding equations reduce to the equation of continuity and the equations of motion in the cylindrical coordinate system. If r tends to infinity in the equations of motion 8, 9, and 10, the terms with a factor of $1/(r^2+a^2)$ or $1/r^n$ $(n=1, 2, 3)$ tend to zero and the terms with a factor of $(r^2+a^2)/r^2$ tend to unity. The equations of motion change from the helical coordinates to the Cartesian coordinate system. This feature will be used to validate the numerical algorithm and computer program in a later section.

No-slip boundary conditions are used in this work:

$$u_{\text{liquid}}=u_{\text{solid}} \qquad v_{\text{liquid}}=v_{\text{solid}} \qquad w_{\text{liquid}}=w_{\text{solid}}. \tag{11}$$

Numerical Method

To simulate flow in helical ducts, a finite difference method is employed to solve the equation of continuity and the equations of motion in unsteady state with the primitive-variable formulation. Some assumptions are made: the liquid in the duct is an incompressible Newtonian fluid. It has constant density, constant viscosity, and constant temperature. The flow in the duct is assumed to be helically symmetrical.

The algorithm used is a modification of the MAC method developed by Welch et al. (1965) and the Project method de-

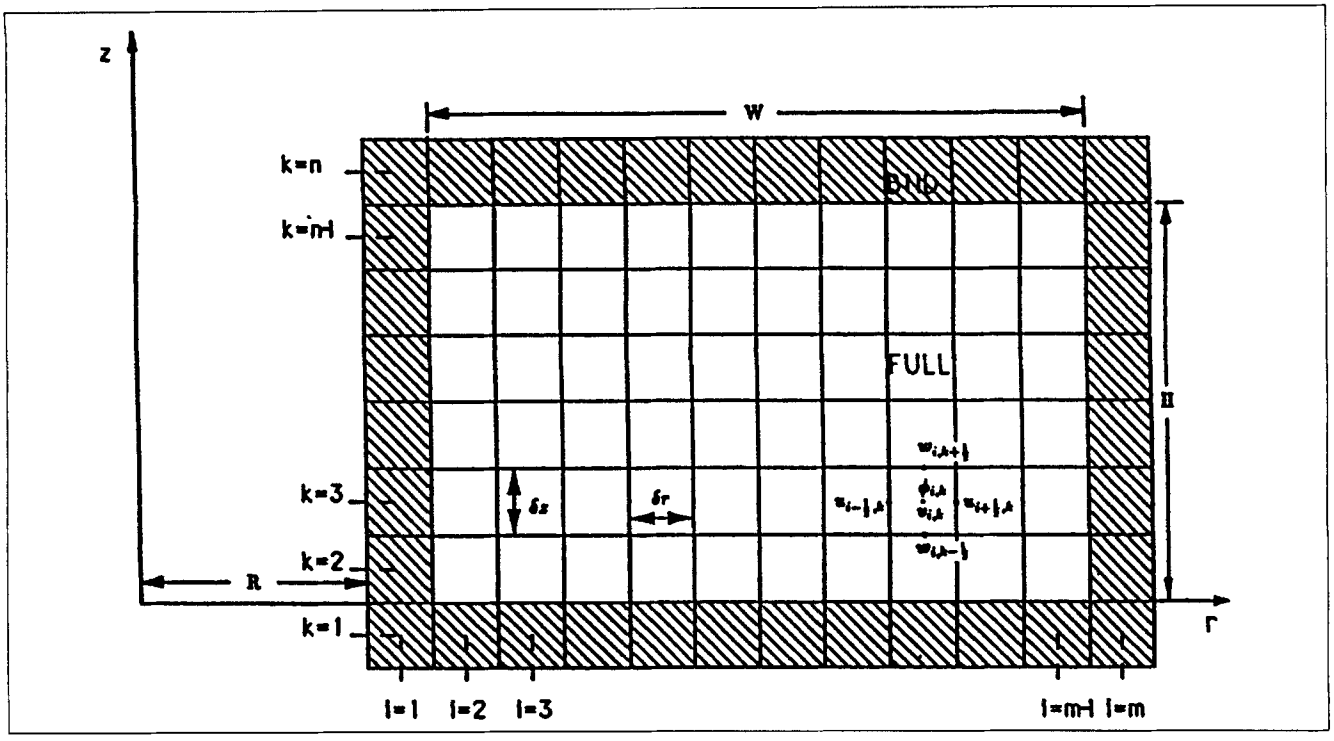

Figure 2. Cell setup and positions of variables.

veloped by Viecelli (1971). At the beginning of every computing cycle, the complete field of velocities is known either from the initial conditions or as a result of the previous cycle of calculations.

The corresponding field of pressures is obtained by solving the Poisson equation for pressure with successive relaxation techniques. According to the pressure changes, the field of velocities is updated.

It is assumed that the velocity field is conservative, which means that the finite difference analogy of velocity divergence vanishes in every cell in the computational region.

The geometry of this helical duct is characterized by the internal radius R, the duct width $2b$, the duct height $2c$, and the duct pitch $2\pi a$. Because the problems in this study are assumed to be helically symmetrical (in the θ direction), the unknowns, u, v, w, p, are functions of t, r, z. The computational region is the cross section of the helical duct. The boundaries of the computational region are defined by the surfaces: $r = R$ and $R + 2b$, $z = 0$ and $2c$, as shown in Figure 2. The computational region is divided into a number of cells, which are defined as boundary cell (BND), which falls outside the system but adjacent to a boundary; full cell (FULL), which contains liquid and is in the computational region. The center of each cell is numbered by the index i, counting the column in the r direction, and the index k, counting the rows in the z direction. The Harlow-Welch staggered-mesh space-differencing scheme is employed in this study, in which the reduced pressure ϕ and velocity v are defined at the center of the cell, the velocities u and w are defined at cell faces.

The flow chart in Figure 3 gives an outline of the computational procedure of this program.

The calculations were performed on a VAX6510 computer. To simulate flow in a straight duct (50×20 mesh), 3,200 time steps and 20 minutes CPU time were needed for the

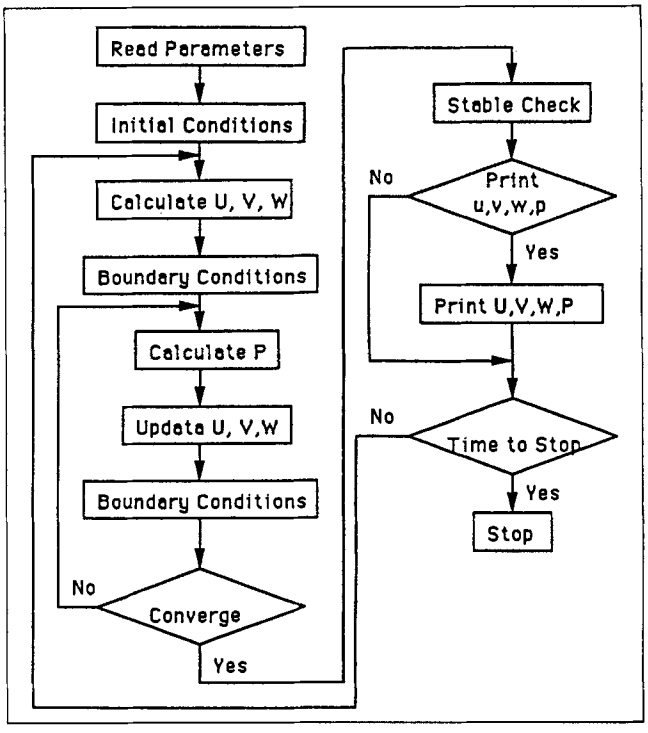

Figure 3. Flow chart of the computer program.

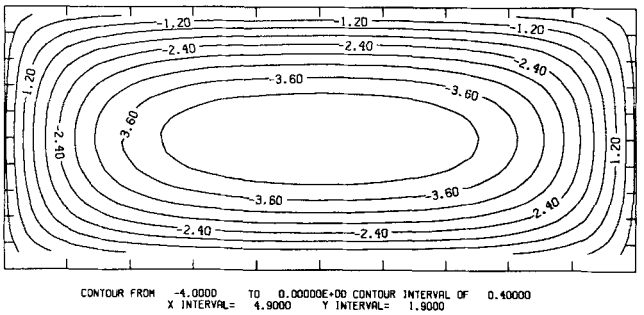

Figure 4. Axial velocity in a straight duct.

program to converge to the required steady flow conditions. To calculate flow in a helical duct, about 2,000 time steps and 10 minutes CPU time were needed.

Validation

If the internal radius R of a helical duct tends to infinity, the helical duct becomes a straight duct. A check on the validity of the numerical method and computer program was made by comparing the numerical simulations of the axial velocities against the analytical solution for flow in a straight duct. The program has been employed to simulate flow in a straight duct by calculating flow in the helical duct in which the internal radius $R = \delta r \times 100{,}000$. The term $\sqrt{r^2+a^2}\,\partial\phi/r^2\partial\theta$ in Eq. 9 is replaced by $d\phi/dy''$, which is perpendicular to the $r-z$ plane; $d\phi/dy''$ is 0.484. The computational region for the whole duct is divided into a 50×20 mesh with each cell 0.1×0.1 in size. The initial conditions are that all velocities equal zero. The no-slip boundary conditions were applied on the solid-liquid boundaries. Other parameters are $\delta t = 0.01$ and $\nu = 0.05$. Five tests of flow in a straight duct were carried out. One of the results is shown in Figure 4. Figure 4 shows very good axially symmetrical contour curves from the left half cross section of the duct to its right half cross section and from the upper half cross section of the duct to its lower half cross section. A similar result is observed when the duct cross section is rotated through 90 degrees.

The axial velocity distribution v in a straight duct with a rectangular cross section, $-b \le r \le b$, $-c \le z \le c$, can be expressed by (Ward-Smith, 1980)

$$v = -\frac{1}{2\nu}\frac{d\phi}{dy''}\left[b^2 - r^2 - \frac{4}{b}\sum_{n=o}^{\infty}\frac{(-1)^n}{N_n^3}\frac{\cosh N_n z}{\cosh N_n c}\cos N_n r\right] \tag{12}$$

where

$$N_n = \frac{(2n+1)\pi}{2b}.$$

Figure 5 shows the comparison of the numerical simulation of axial velocities with the analytical solution in columns 1, 5, 10, 15, 20, and 25 in the computational region. In Figure 5,

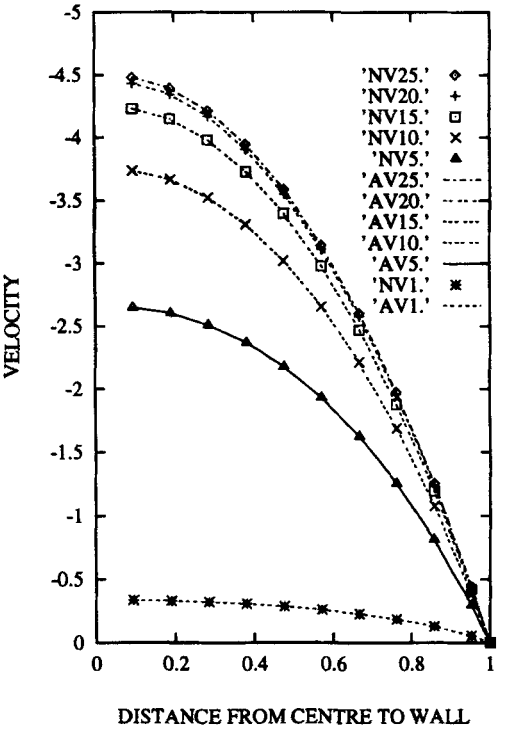

Figure 5. Analytical solution vs. numerical simulation.

"NV" indicates that results are from a numerical simulation and "AV" indicates that results are calculated from the analytical solution. The digits after "NV" or "AV" represent the number of the column in the computational region. Column 1 is the first column close to the solid wall boundary and Column 25 is the central column in the computational region. The highest velocities are located at the center of the duct, while all velocities are necessarily zero at the wall of the duct. Figure 5 shows that agreement is excellent as expected.

According to Figure 4 and Figure 5, the numerical simulations of flow in a helical duct with internal radius R tending to infinity match the analytical solutions of flow in a straight

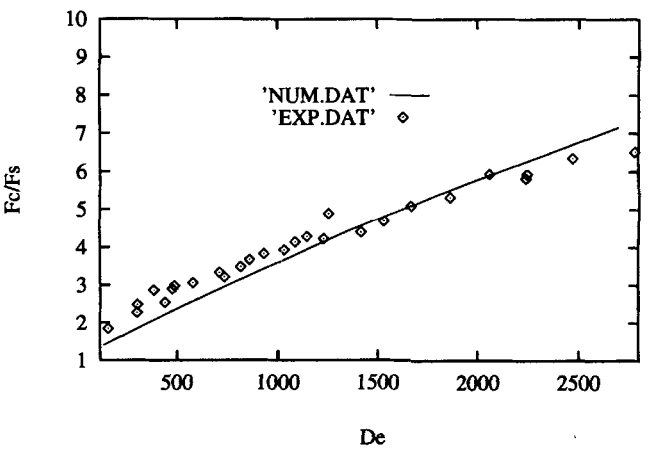

Figure 6. Numerical simulation vs. experimental measurement of flow resistance.

duct, which indicate that the algorithm, the discretized equations, boundary conditions, and computer program are appropriate for simulating duct flow.

General Helical Duct

Secondary flow is the main feature of flow through a curved pipe and duct, which is caused by the centrifugal force due to the curved boundaries. Dean (1928) defined a dimensionless number, the Dean number De, to show the ratio between inertial force and viscous force, and between hydraulic diameter and internal radius.

The hydraulic diameter D_h, cross-section shape-factor γ, curvature ratio λ, pitch ratio P_r, Reynolds number Re, Dean number De, friction-factor for a straight duct with a rectangular cross-section Fs, and friction-factor for a helical duct with a rectangular cross-section Fc are defined as

$$D_h = \frac{4bc}{b+c} \qquad \gamma = \frac{c}{b} \qquad \lambda = \frac{D_h}{4R} \qquad P_r = \frac{\text{Pitch}}{R}$$

$$Re = \frac{D_h v}{\nu} \qquad De = Re\sqrt{\lambda} \qquad Fs = \frac{Cs}{Re} \qquad Fc = \frac{2D_h}{\rho v_m^2}\frac{\Delta P}{\Delta s}$$

where $2b$ and $2c$ are the width and height of the rectangular cross section of the helical duct, respectively, R is the internal radius of the helical duct, and v_m is the mean helical

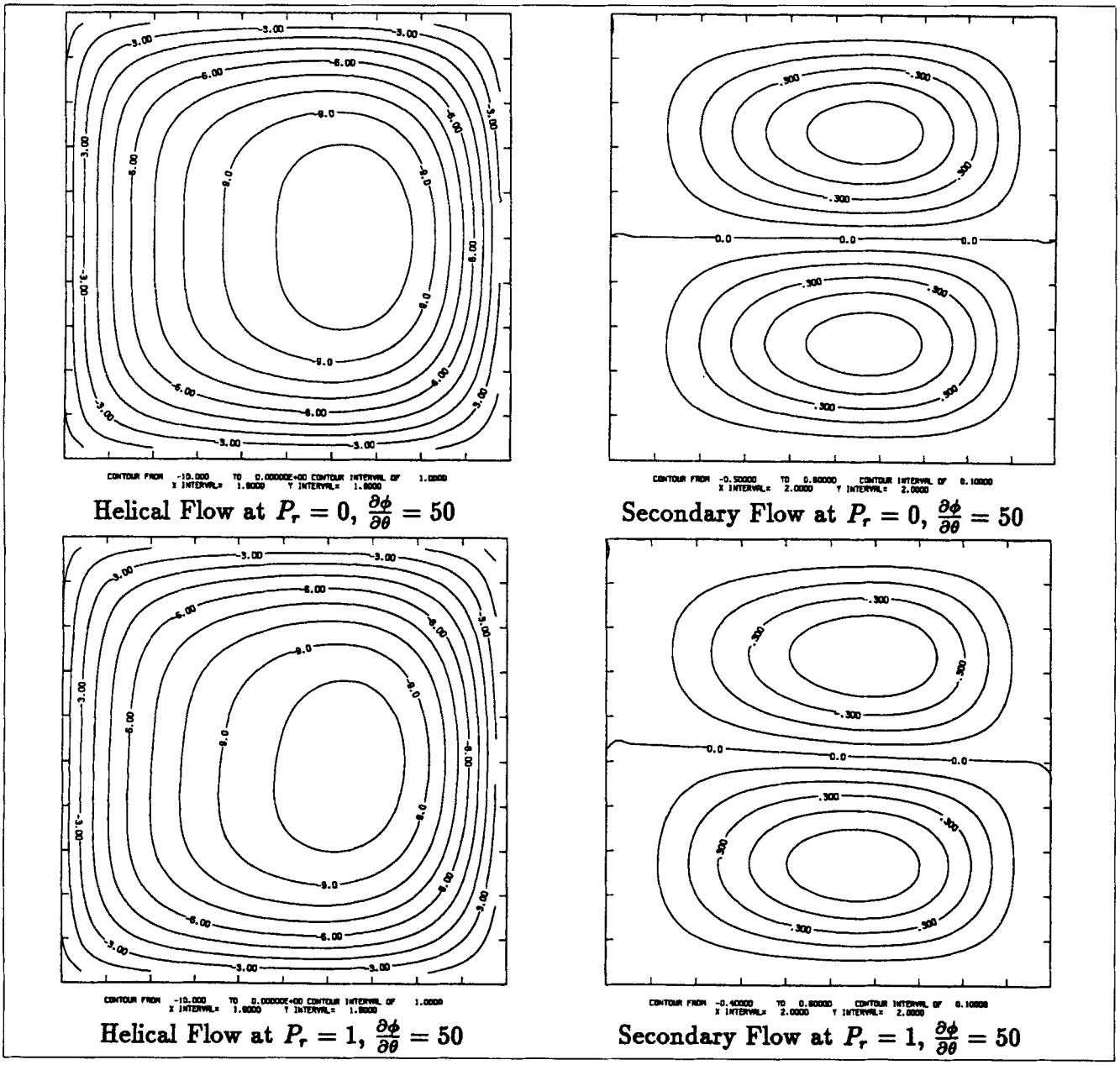

Figure 7. Effect of pitch ratio P_r on helical flow and secondary flow.

velocity. Ward-Smith (1980) suggested that $Cs = 57$ if $\gamma = 1$, $Cs = 62.2$ if $\gamma = 2$ or $\gamma = 0.5$.

Sixteen cases have been simulated. The computing region was 20×20 cells. The other parameters were cell dimensions $\delta r = \delta z = 0.05$, time interval $\delta t = 0.005$, radius of curvature $R = \delta r \times 190$, pitch = 31, viscosity $\nu = 0.1$, overrelaxation parameter $\omega = 1.7$.

The initial conditions were that all velocities were zero. The no-slip boundary conditions were applied on the four walls of the duct.

Huang and Gu (1989) carried out some experiments to measure the pressure drop variation as a function of the flow rate in a helical duct of rectangular cross section. Figure 6 compares the numerical simulations generated by this method with data based on Huang's experiments. The figure shows that relative friction-factor Fc/Fs increases with the Dean number De for flow through a helical duct with a rectangular cross section. While the numerical simulation results and the experimental results of Huang and Gu are not identical, they are similar, although the experimental results appear to lie on a curve with a smaller gradient. (There is a paucity of experimental data for these conditions and additional studies are badly needed.)

Because the centrifugal force intensifies the motion of the fluid particles in a curved pipe or duct, the friction of flow in the curved pipe or duct is higher than that in a straight pipe

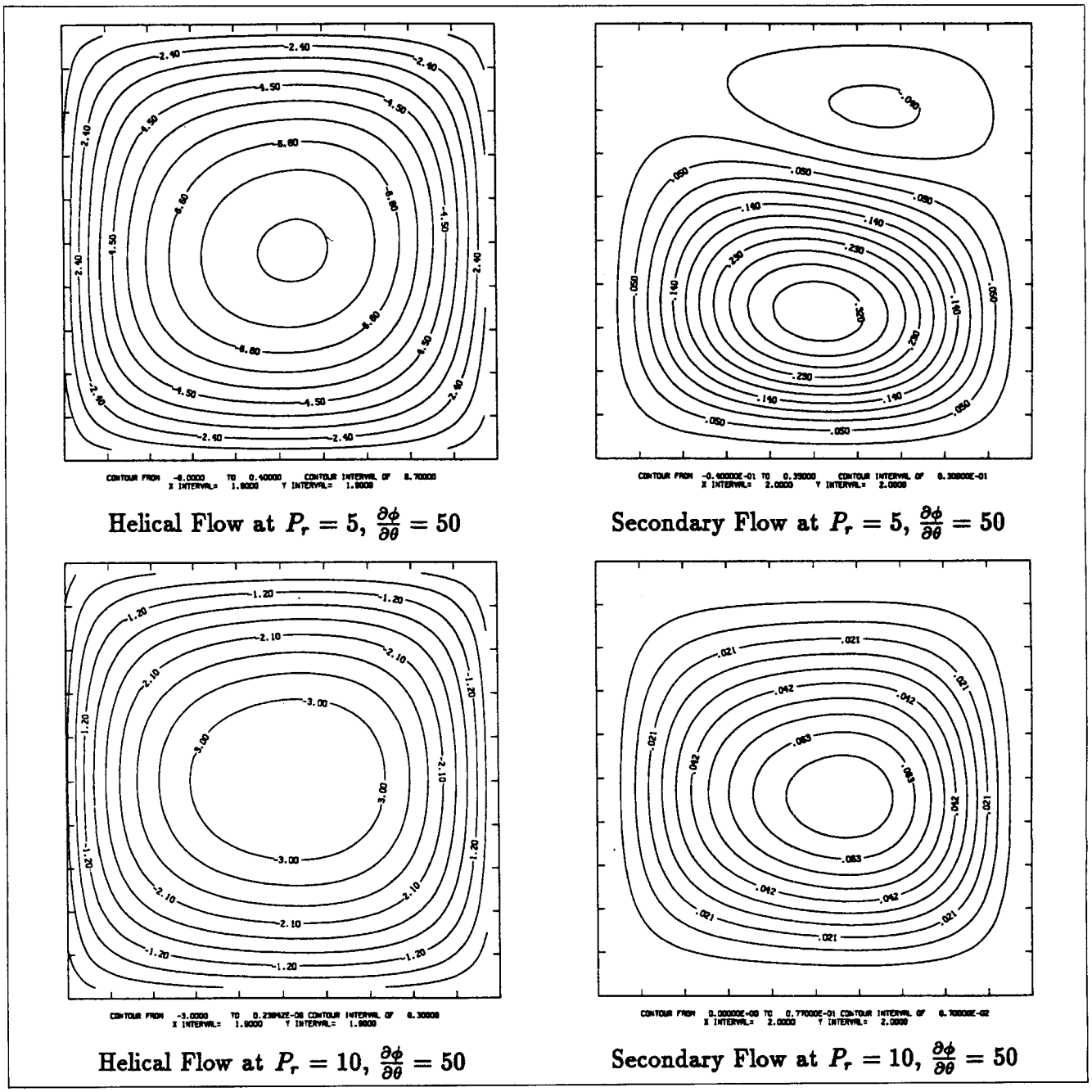

Figure 8. Effect of pitch ratio P_r on helical flow and secondary flow.

or duct. The factors that will affect the secondary flow and flow resistance in a helical duct are the pitch ratio P_r, pressure gradient $\partial\phi/\partial\theta$, and curvature ratio λ.

Effect of pitch ratio P_r

A series of simulations were run to ascertain how the pitch of a helical duct affects the secondary flow and the helical flow in a helical duct. In all cases the pressure gradient $\partial\phi/\partial\theta$ was set at 50. The pitch ratio P_r was varied from 0 to 10.

Secondary flow is displayed by means of the stream function, which is the combination of the radial velocities and the vertical velocities. Figures 7 and 8 show four sets of helical velocity and stream function data on the cross section of the helical duct. When the pitch ratio P_r is equal to zero, the helical duct becomes a toroidal duct. The highest helical velocity is located at the middle between the upper and lower boundaries of cross section of the duct. Because of centrifugal force, the highest helical velocity is pushed toward the outer vertical wall of the duct, as shown in Figures 7 and 8. The major difference between a flow in a toroidal duct and a flow in a helical duct is that a pair of symmetrical secondary vortexes appears on the cross section of a toroidal duct. But the secondary vortexes on the cross section of a helical duct are not symmetrical. As shown in Figures 7 and 8, when pitch ratio P_r is greater than zero, the lower vortex becomes bigger and the upper vortex becomes smaller, which means that the intensity of secondary flow in the upper part of the cross section of the duct is getting weaker and the intensity of the secondary flow in the lower part of the cross section is getting stronger. Figure 8 also shows that the upper vortex disappears completely and the lower vortex occupies the entire cross section of the helical duct when P_r is equal to 10. These results lead to a different conclusion from that obtained by Joseph et al. (1975), who found that the twin rotating currents occur at all Dean numbers in helical ducts. The reason for the different conclusion is that Joseph used a toroidal coordinate system to simulate flow in a helical duct. No pitch effects were shown in his simulations. As mentioned earlier, there is an extra acceleration term $2auv/(r\sqrt{r^2+a^2})$ in the third equation of motion in a helical coordinate system, which does not appear in the equations of motion in a cylindrical or toroidal coordinate system. This acceleration term may cause

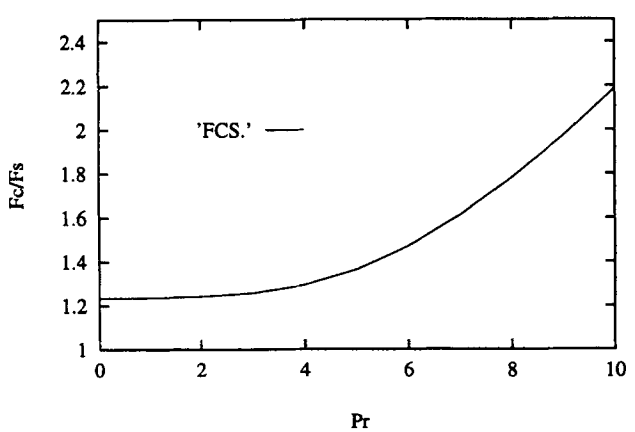

Figure 9. Effect of pitch ratio P_r on resistance of flow.

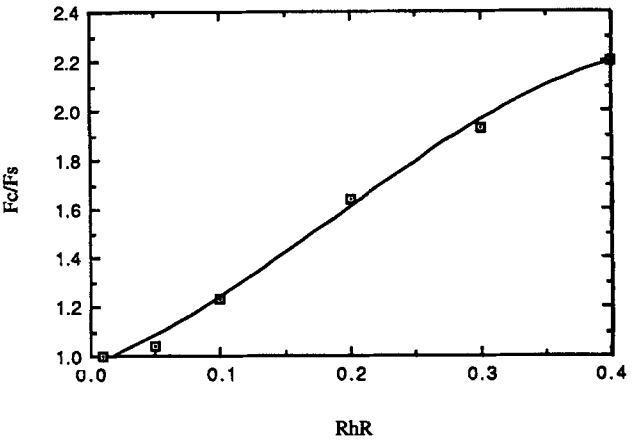

Figure 10. Effect of curvature ratio λ on resistance of flow.

the lower vortex to become greater and to occupy the whole cross section of the duct.

The pitch ratio P_r not only affects the secondary flow, but also the resistance of flow in a helical duct. Figure 9 shows that the relative friction-factor of flow Fc/Fs increases with the pitch ratio P_r.

Effect of curvature ratio λ

The relative friction-factor of flow Fc/Fs in a helical duct mainly depends on the curvature ratio λ because of centrifugal force. For a helical duct with a constant hydraulic diameter D_h, if the radius of the helix is small, the centrifugal force and the curvature ratio λ become great; if the helical radius is large, the centrifugal force and curvature ratio become small. The relative friction-factor Fc/Fs increases or decreases with the centrifugal force and curvature ratio λ. The limiting case is that if the radius of the helix tends to infinity, the helical duct becomes a straight duct. The curvature ratio λ and centrifugal force become zero and the relative friction-factor Fc/Fs reduces to unity for flow in a straight duct. A series of numerical calculations was carried out with the same conditions and same hydraulic diameters as were

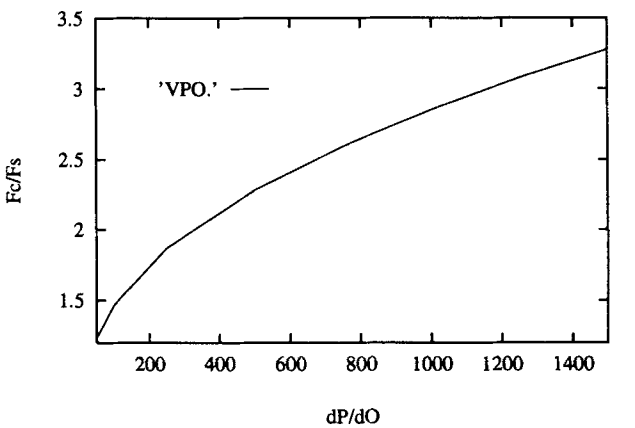

Figure 11. Effect of pressure gradient $\partial\phi/\partial\theta$ on resistance of flow.

used previously. The curvature ratio λ, however, was varied from 0.01 to 0.4. Figure 10 shows that when λ equals 0.4, *Fc/Fs* equals 2.201. When λ equals 0.01, *Fc/Fs* equals 1.002. Also, *Fc/Fs* in a helical duct decreases with the curvature ratio λ. The effect of the curvature ratio is accounted for mainly in relative friction-factor of flow *Fc/Fs*, but with slight effect on the secondary flow.

Effect of pressure gradient $\partial\phi/\partial\theta$

Because the helical velocity and secondary flow increase as the pressure gradient $\partial\phi/\partial\theta$ increases, the pressure gradient has a large influence on the relative friction-factor of flow and the secondary flow in a helical duct. Ten simulations were conducted. Again, the same conditions as were used before were used except the pressure gradient $\partial\phi/\partial\theta$ was varied from 50 to 2,300. As the pressure gradient increased, the flow increased and the secondary flow patterns become more intense. The relative friction-factor *Fc/Fs* increased with the pressure gradient $\partial\phi/\partial\theta$ in the helical duct (Figure 11).

Figure 12 shows helical velocities and secondary flow change with the pressure gradient. The Dean number increases with the pressure gradient. When the Dean number is increased to a certain level (the transitional Dean number), a pair of weaker secondary flow vortexes appear close to the outer wall. Four vortexes are in the cross section of the helical duct when P_r is equal to 1 and $\partial\phi/\partial\theta$ equals 2,300 (Figure 12).

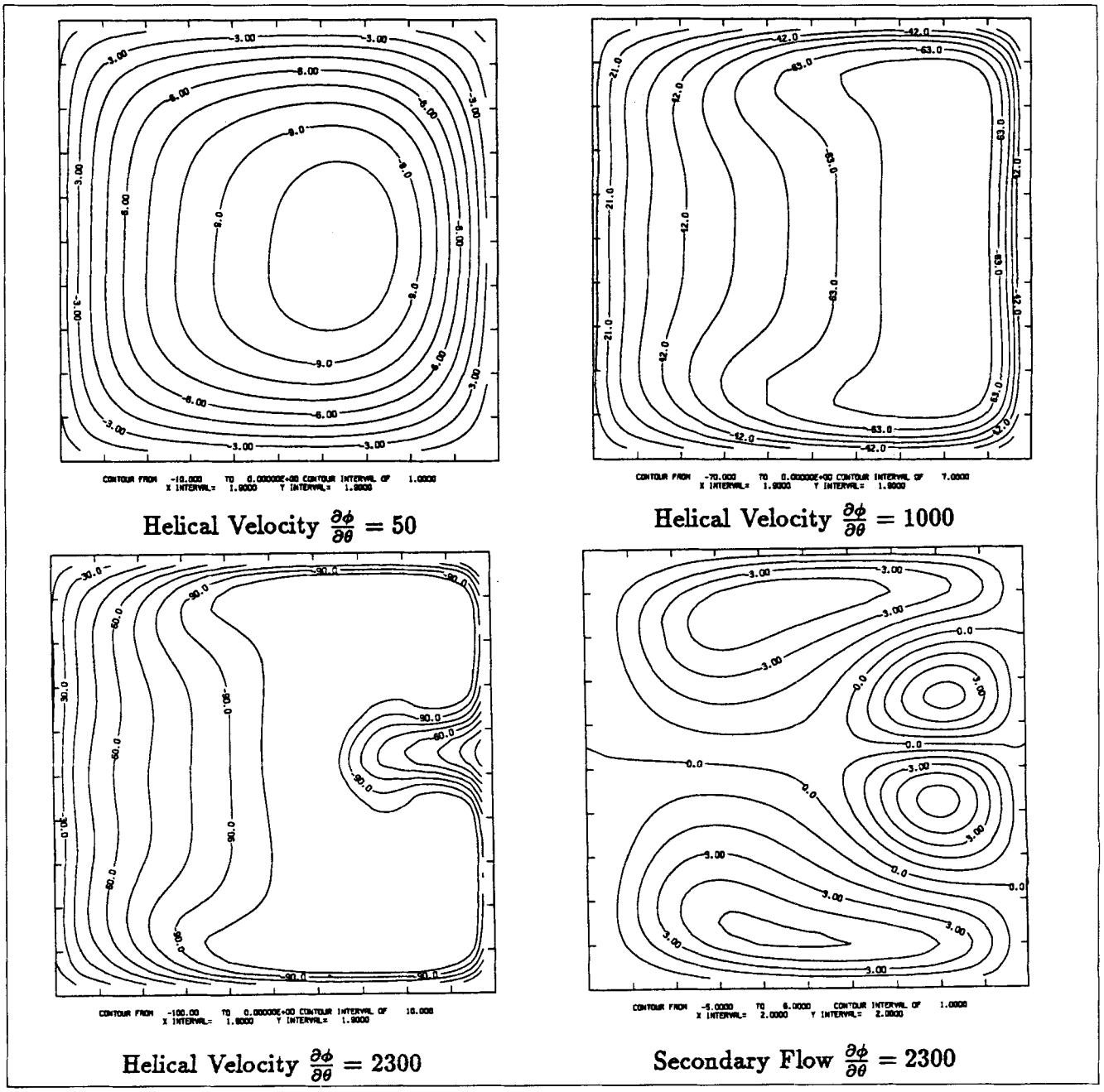

Figure 12. Effect of pressure gradient on helical flow and secondary flow.

Conclusions

Secondary flow and a higher flow friction are the main features of fluid flow in a helical duct. These have been studied using the motion equations and the continuity equation solved numerically for fully developed, incompressible, viscous Newtonian flow in a helical duct with square or rectangular cross section. Twenty-nine cases were simulated to cover pitch ratios from 0 to 10, curvature ratios from 0.01 to 0.4, pressure gradients from 50 to 2,300, cross-section shape factors from 0.5 to 2, and Dean numbers from 0.69 to 244. The following conclusions can be drawn concerning flow in a helical duct:

(a) The pitch ratio of a helical duct affects the pattern of the secondary flow and the relative friction-factor. Two vortexes will become a single vortex if the pitch ratio is greater than 10. The relative friction-factor increases as pitch ratio increases.

(b) The relative friction-factor is affected mainly by the curvature ratio.

(c) The pressure gradient has a large influence on the secondary flow and flow resistance. When the pressure gradient reaches a certain level, there are four vortexes that appear on the plane of the cross section. The relative friction-factor is increased with pressure gradient.

Acknowledgment

The authors are very grateful to Professor Frank Lawson and Mrs. Jill Anderson, both of Monash University, for reading the manuscript and providing valuable suggestions. Also, the financial support received from Minpro Pty Ltd., in Australia is gratefully acknowledged.

Notation

a = constant in helical coordinates, Pitch/2π, dimensionless
b = half-width of the rectangular cross section of the helical duct, dimensionless
c = half-height of the rectangular cross section of the helical duct, dimensionless
c_u = curvature, $c_u = R/(R^2 + a^2)$, dimensionless
D_h = hydraulic diameter of the duct, $D_h = 4bc/(b + c)$, dimensionless
$D_{i,k}$ = divergence of the liquid velocity
Fc = friction-factor for a helical duct with a rectangular cross section
Fs = friction-factor for a straight duct with a rectangular cross section
f^i = gravity acceleration in i direction, cm/s^2
$\mathbf{g}$ = gravity acceleration, cm/s^2
g_c = acceleration, constant, cm/s^2
g_r = gravity acceleration in r direction, dimensionless
g_θ = gravity acceleration in θ direction, dimensionless
g_z = gravity acceleration in z direction, dimensionless
$\mathbf{g}_i$ = covariant base vectors
$\mathbf{g}^i$ = contravariant base vectors
g_{ij} or g^{ij} = metric tensory, Eq. 2
L' = characteristic length, cm
p = pressure, dyne/cm^2
Pitch = pitch for a helical duct, dimensionless
P_r = pitch ratio, P_r = Pitch/R, dimensionless
r = r coordinate in helical coordinate system
δr = r increment, dimensionless
R = distance from z coordinate to nearest vertical boundary of duct, dimensionless
t = time, dimensionless
δt = time increment, dimensionless
t_o = torsion, $t_o = a/(a^2 + R^2)$, dimensionless
u = velocity in r direction, dimensionless
$\mathbf{v}$ = vector of velocity, dimensionless
v = velocity in θ direction, dimensionless
v^i = vector component
$v^{(i)}$ = physical component of the vector $\mathbf{v}$
v_m = mean helical velocity, dimensionless
w = velocity in z direction, dimensionless
x'' = x coordinate in Cartesian coordinate system
x^i = i coordinate in a coordinate system
X^i = helical coordinate system
y'' = y coordinate in Cartesian coordinate system
Y^i = Cartesian coordinate system
z = z coordinate in helical coordinate system
z'' = z coordinate in Cartesian coordinate system
δz = z increment, dimensionless

Greek letters

γ = cross-section shape factor c/b
λ = curvature ratio $\lambda = D_h/R$
θ = θ coordinate in helical coordinate system
ν = kinematic viscosity, cm^2/s or dimensionless
ρ = density, g/cm^3
ϕ = ratio of pressure to density, $\phi = p/\rho$, dimensionless
ω = overrelaxation parameter

Literature Cited

Aris, R., *Vectors, Tensor, and the Basic Equations of Fluid Mechanics*, Prentice-Hall, International, London (1962).

Austin, L. R., and J. D. Seader, "Fully Developed Viscous Flow in Coiled Circular Pipes," *AIChE J.*, **19**, 85 (1973).

Berger, S. A., L. Talbot, and L.-S. Yao, "Flow in Curved Pipes," *Annu. Rev. Fluid Mech.*, **15**, 461 (1983).

Browne, L. W. B., "The Marker And Cell Technique," *Numerical Simulation of Fluid Motion*, North-Holland, Amsterdam (1978).

Dean, W. R., "Note on the Motion of Fluid in a Curved Pipe," *Phil. Mag. Ser.*, **4**, 208 (1927).

Dean, W. R., "The Stream-line Motion of Fluid in a Curved Pipe," *Phil. Mag. Ser.*, **5**, 673 (1928).

Eringen, A. C., *Mechanics of Continua*, Wiley, New York (1967).

Germano, M., "On the Effect of Torsion on a Helical Pipe Flow," *J. Fluid Mech.*, **125**, 1 (1982).

Germano, M., "The Dean Equations Extended to a Helical Pipe Flow," *J. Fluid Mech.*, **203**, 289 (1989).

Huang, W., and D. Gu, "A Study of Secondary Flow and Fluid Resistance in Rectangular, Helical Coiled Channel," *Int. Chem. Eng.*, **29**, 480 (1989).

Ito, H., "Review, Flow in Curved Pipes," *JSME Int. J.*, **30**, 543 (1987).

Joseph, B., E. P. Smith, and R. J. Adler, "Numerical Treatment of Laminar Flow in Helically Coiled Tubes of Square Cross Section," *AIChE J.*, **21**, 965 (1975).

Joseph, B., and R. J. Adler, "Oscillating Helically Coiled Tubes," *AIChE J.*, **21**, 974 (1975).

Kao, H., "Torsion Effect on Fully Developed Flow in a Helical Pipe," *J. Fluid Mech.*, **184**, 335 (1987).

Viecelli, J. A., "A Computing Method for Incompressible Flows Bounded by Moving Walls," *J. Comput. Phys.*, **4**, 119 (1971).

Wang, C. Y., "On the Low-Reynolds-Number Flow in a Helical Pipe," *J. Fluid Mech.*, **8**, 185 (1981).

Ward-Smith, A. J., "Internal Fluid Flow," in *The Fluid Dynamics of Flow in Pipes and Ducts*, Clarendon, Oxford (1980).

Welch, J. E., F. H. Harlow, J. P. Shannon, and B. J. Daly, "The MAC Method: A Computing Technique for Solving Viscous, Incompressible, Transient Fluid Flow Problems Involving Free Surface," Los Alamos Scientific Laboratory Report, No. LA-3425 (1966).

Manuscript received Dec. 13, 1993, and revision received Apr. 4, 1994.